ELSEVIER

Polymer 42 (2001) 3489–3502

polymer

www.elsevier.nl/locate/polymer

Compatibilization and properties of PBT/PU polymeric alloys

P.S. Archondouli, N.K. Kalfoglou*

Department of Chemistry, University of Patra, 26500 Patra, Greece

Received 18 July 2000; received in revised form 25 September 2000; accepted 16 October 2000

Abstract

Melt mixed blends of poly(butylene terephthalate) (PBT) with a polyester type polyurethane (PU) were characterized by tensile testing, dynamic mechanical analysis (DMA), differential scanning calorimetry (DSC), optical and electronic microscopy (SEM) and solution ^{1}H NMR. Blends prepared covered the complete composition range. Large deformation behavior, thermal properties and DMA indicated partial component mixing and mechanical compatibility typical of a polymeric alloy. Morphology examination revealed good component dispersion and strong interface adhesion. ^{1}H NMR of blends showed the formation of a PBT–PU copolymer by ester–amide interchange reactions whose extent depended on the PBT–PU ratio and melt mixing conditions. Evidence for the formation of the copolymer was also provided by FT-IR. This in situ formed copolymer is responsible for the compatibilization achieved.

Keywords: PBT/PU alloys; In situ compatibilization; Blend characterization

1. Introduction

In a recent work [1] the in situ compatibilization of poly(ethylene terephthalate) (PET) with a polyester type polyurethane (PU) was studied. It was established by ^{1}H NMR that at the melt mixing conditions applied, an in situ PET–PU copolymer was formed via ester–amide interchange reactions. This reactive compatibilization accounts for the mechanical, thermal and morphological properties observed in these polymeric alloys.

The present study is an extension of the above work and examines the compatibilization of poly(butylene terephthalate) (PBT)/PU blends. PBT is an easily crystallizable main chain aromatic polyester and inclusion of PU is expected to improve its impact strength. It was also of interest to examine whether a reactive compatibilization via a similar mechanism as before would be obtained during melt mixing.

Related past work on aromatic polyesters/PU blends dealt primarily with the polycarbonate (PC)/PU pair. In solution with cyclohexanone, polyester or polyether type PU was stated to be incompatible [2]. Melt mixing may lead to miscible or compatible polymer blends as the work of Fabri et al. [3] demonstrated for PU elastomers based on 4,4′-diphenylmethane diisocyanate (MDI) and aliphatic polycarbonate diols and/or butanediol-1,4 (BD-1,4). Miscibility was attributed to hydrogen bonding interactions between the –NH of the PU and the –C=O of the polyester. Analogous findings were reported by Ahn et al. [4] on similar blends. The PU component was based on MDI, BD-1,4 as the hard segment and poly(ethylene adipate) or poly(butylene adipate) as the soft segment. Solvent cast films annealed in the differential scanning calorimeter (DSC) between 230 and 270°C for various periods of time showed convergence of the main components' T_gs. This was taken as evidence for reactive compatibilization attributed to ester–amide interchange reactions.

Very little work on aliphatic polyester/PU blends was found in the literature. Poly(methyl methacrylate)/PU blends consisting of linear homopolymers or prepolymers capable of forming interpenetrating networks were examined by Kim et al. [5,6]. In solvent cast films distinct phase separation and component T_g invariance were reported for the linear polymer blends while there was limited T_g convergence for the interpenetrating system and results from electron microscopy also indicated incompatibility but with a finer distribution of the dispersed phases.

Analogous findings were reported by Kwei, Frisch and coworkers [7], who examined the morphology and dynamic viscoelastic properties of interpenetrating networks based on polyacrylate/urethane–urea prepolymers.

In the present work compatibility characterization was carried out on blends covering the complete composition range. Techniques applied were tensile testing, DSC, dynamic mechanical analysis (DMA), optical microscopy, FT-IR, electron microscopy (SEM) of cryofractured and etched specimens, and ^{1}H NMR.

* Corresponding author. Tel.: +30-61-997-102; fax: +30-61-997-122.
E-mail address: n.kalfog@chemistry.upatras.gr (N.K. Kalfoglou).

0032-3861/01/$ - see front matter
PII: S0032-3861(00)00758-8

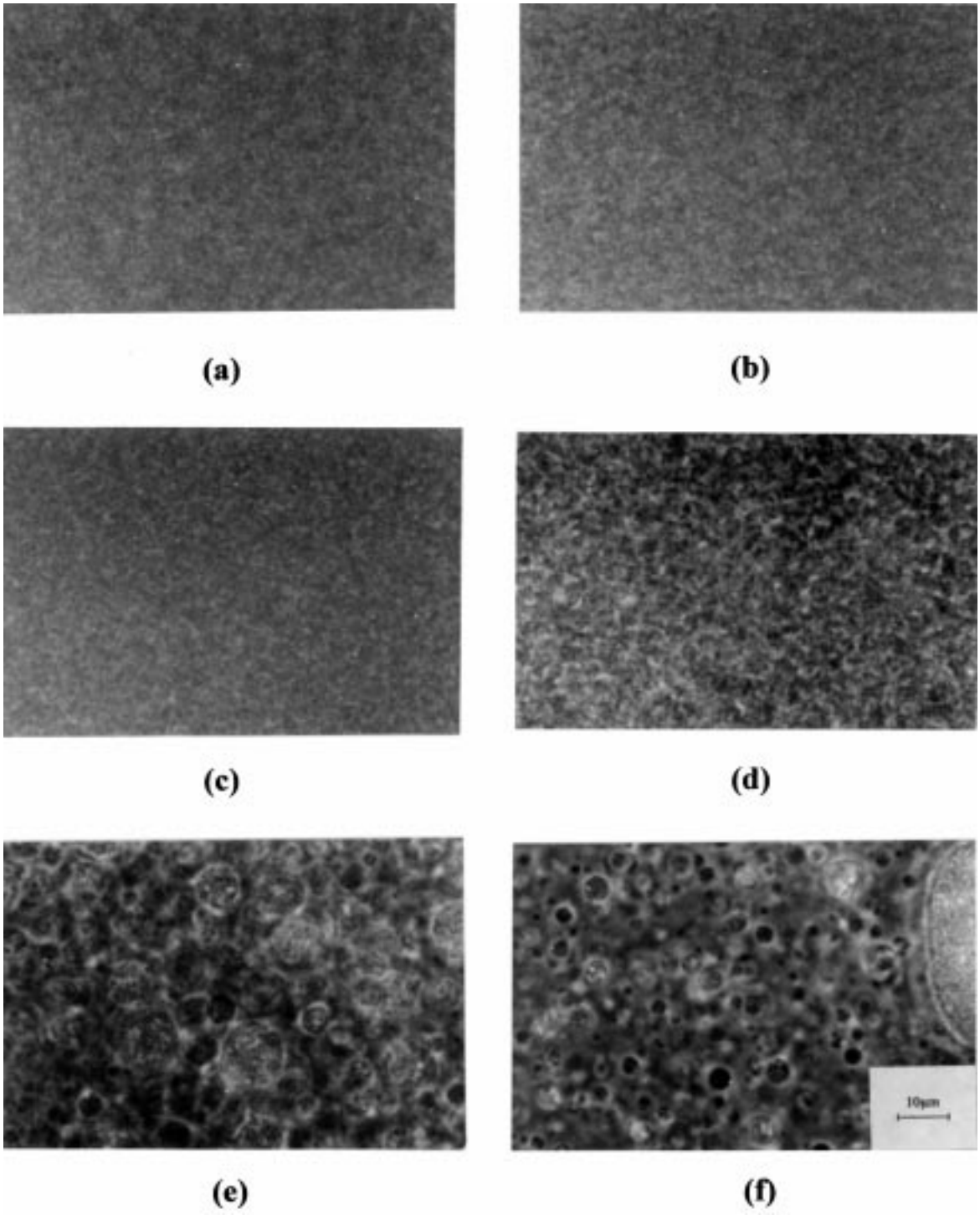

Fig. 1. Phase contrast micrographs of PBT/PU blends: (a) 100/0; (b) 90/10; (c) 75/25; (d) 50/50; (e) 25/75; (f) 10/90.

2. Experimental

2.1. Materials and specimens preparation

PBT used was obtained from Nevicolor SpA, Italy. It is an injection molding grade with density 1.31 g cm^{-3} and MFI 35 (250°C, g/10 min). PU (Desmopan 359) was donated by Bayer A.G. It is a polyester type PU with hard segments formed by the addition of BD-1,4 to MDI. The soft segment, with M_n of ca. 2000 g mol^{-1} consists of polyester chains formed by polycondesation of adipic acid and BD-1,4. Density was 1.23 g cm^{-3}. PU was dried at 100°C for 24 h and PBT at 110°C for 5 h, in dynamic vacuo. The dried materials were blended at ca. 250°C under a blanket

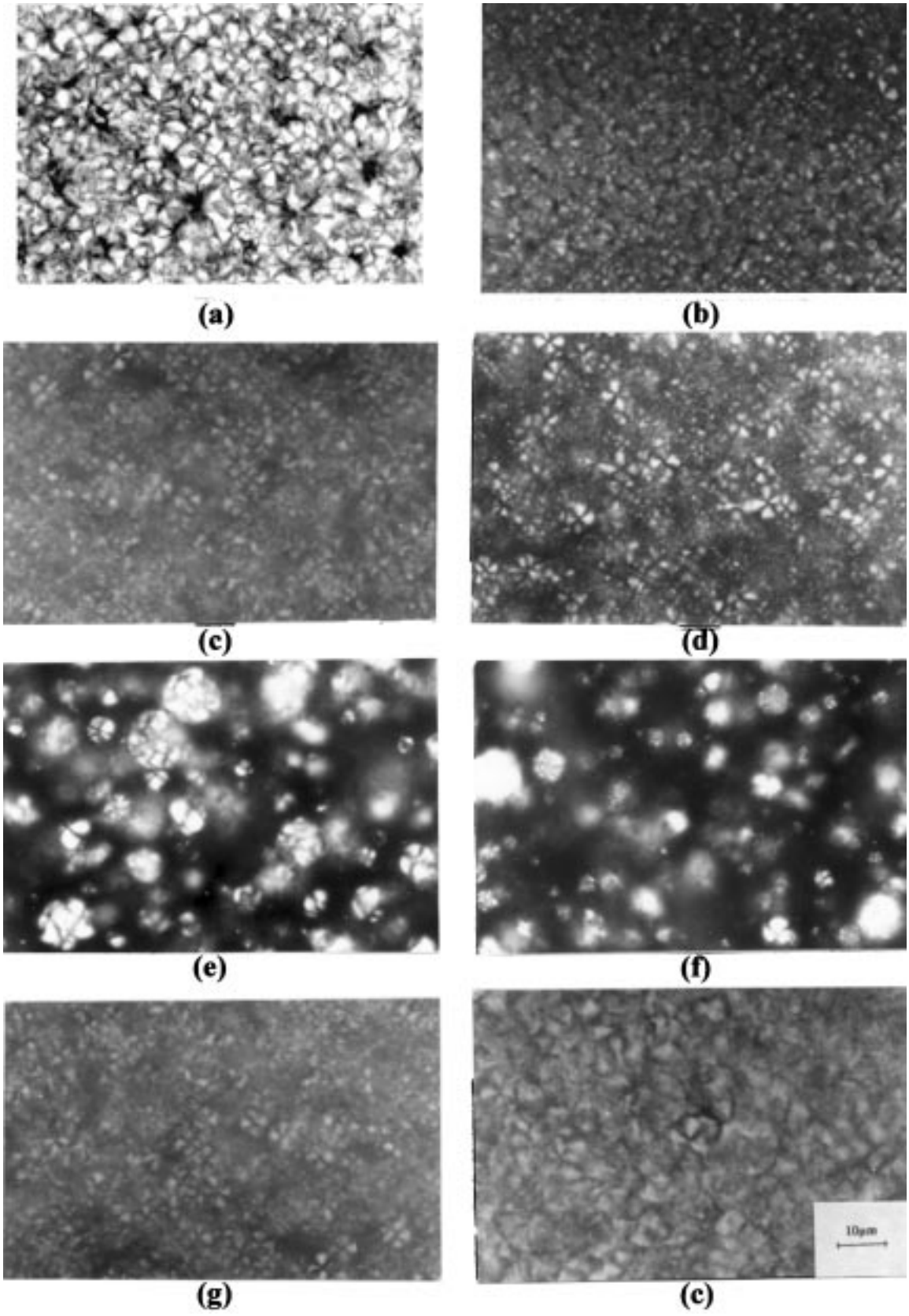

Fig. 2. Optical micrographs with crossed polars of PBT/PU blends: (a) 100/0; (b) 90/10; (c) 75/25; (d) 50/50; (e) 25/75; (f) 10/90; (g) quenched 75/25; (h) annealed 75/25.

of inert gas (Ar) in a home-made stainless steel bob-and-cup type of mixer previously described [8]. PBT/PU compositions prepared were 90/10, 75/25, 50/50, 25/75, 10/90 (w/w).

Films were obtained by compression molding between Teflon sheets at ca. 250°C and 5 MPa, followed by quenching to 0°C.

2.2. Apparatus and procedures

Tensile tests were performed at 23°C, according to ASTM D882 at a crosshead speed of 10 cm min^{-1} using a J.J. Tensile Tester Type 5001 and film strips measuring $3.00 \times 0.65 \times 0.025$ cm^3.

DSC measurements were carried out using the DSC (SP +) equipped with the Autocool accessory from Rheometric Scientific Co. Sample weight was ca. 10 mg and the thermal cycling applied for the crystallinity determination of blends was 25 → 250°C with 20°C heating rate, quenching to −60°C and heating up to 250°C with 10°C min^{-1}. The second heating run was recorded. All the experiments were performed under a constant flow of dry nitrogen.

DMA data were obtained at 10 Hz with the RSA II mechanical spectrometer from Rheometric Scientific Co. Specimen dimensions were $3.0 \times 0.5 \times 0.01$ cm^3.

Examination of the effects of possible ester–amide interchange reactions was performed by means of high resolution solution ^{1}H NMR spectroscopy. Spectra were measured with an Avance DPX 400 MHz with a magnetic field strength of 9.4 T. The samples were dissolved in a 2/1 (v/v) mixture of trifluoroacetic acid and deuterated chloroform, to obtain 5 wt% solutions.

Optical micrographs with phase contrast and crossed polar arrangements were obtained with an Olympus BH-2 microscope.

SEM was carried out on a JEOL model JSM-500 instrument. Cryofractured or etched surfaces were examined at a tilt angle of 0°.

Selective leaching of PU was carried out using dimethylformamide (DMF) (6 days at ambient temperature).

FT-IR spectra were obtained using a Perkin–Elmer 1600 spectrometer.

3. Results

3.1. Morphology

3.1.1. Optical microscopy

Phase contrast may reveal blend heterogeneity since $\eta^D_{PU} = 1.550$ [9] and $\eta^D_{PBT} = 1.587$; the latter was calculated [10] using formulas suitable for semicrystalline polymers. At positive phase contrast dark areas should correspond to PBT. The effect of composition variation is shown in Fig. 1. Increasing PU content leads to a coarser phase distribution and at compositions ≥50/50, PBT is dispersed as spherical globules (containing PU inclusions) in a PU matrix. A similar composite morphology was also obtained in PET/PU blends [1]. Polarizing microscopy confirms these findings; see Fig. 2. The effect of annealing is also shown in Fig. 2(g) and (h) for one composition, 75/25. The main effect is the increase of the spherulite size of PBT. The effect of t_{mix} is revealed in Fig. 3. Increasing t_{mix} results in improved dispersion (Fig. 3(a) and (b)). At increased PU levels a t_{mix} increase leads to the progressive development of composite PBT globules with a concomitant decrease of uniformity in dispersion; Fig. 3(c)–(e).

3.1.2. SEM

Additional information on morphology and phase adhesion is provided by SEM. Cryofractured specimens show a mixed ductile–glassy fracture at high and medium PBT levels; see Fig. 4. This characterizes a high degree of phase adhesion in a heterogeneous blend. For phase separated and poorly adhering phases after fracture one would obtain smooth circular craters where the minor component was occluded into the matrix. Fracture at ambient temperature yields a fibrillar texture since both strongly attached components may easily elongate: the PU by elastic deformation, the PBT by cold drawing; see Fig. 5(a)–(c). A similar morphology was obtained for PET/PU blends only at increased PU levels [1]. This is attributed to the higher $T_{g,PET}$. Leaching out PU reveals the PBT matrix formed at increased PBT levels — Fig. 6(a), the interpenetrating component distribution at the median composition — Fig. 6(b) and the spherical PBT composite inclusions at higher PU contents — Fig. 6(c).

3.2. Tensile properties

The results and their standard deviation of tensile testing are summarized in Table 1 in terms of strength σ_b, yield stress σ_y, elongation % at break ϵ_b, and energy to tensile failure E_b; the last quantity is related to impact tensile strength.

These ultimate tensile behavior results, especially ϵ_b, indicate good interphase component adhesion typical of a polymeric alloy. Significant PBT impact improvement is achieved with the addition of 25–50 wt% PU. Table 1 indicates that $t_{mix} \geq 5$ min is adequate though optical microscopy indicated improved dispersion at $t_{mix} \cong 10$ min. Further increase of t_{mix} may be detrimental to tensile properties — possibly the result of PU decomposition as TGA data have shown. Aging affects the properties in PBT-rich compositions. This could be the result of PBT crystallinity increase that may proceed at room temperature [11]. Annealing affects mechanical properties adversely not because of PBT crystallinity increase (see Table 2), but because of enhanced PBT spherulitic growth, as optical microscopy indicated and because of an increased level of phase separation; see above.

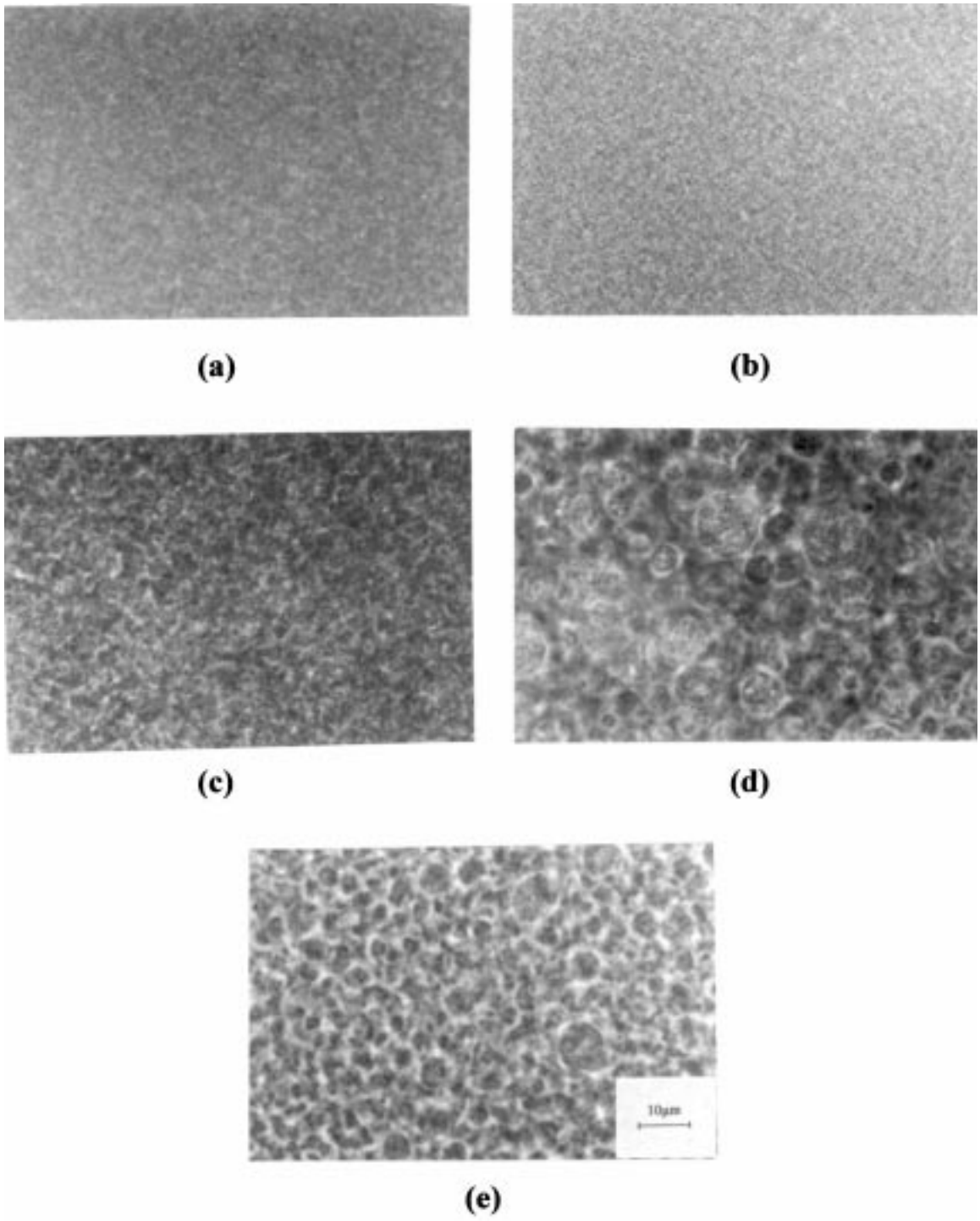

Fig. 3. Phase contrast micrographs of PBT/PU blends. Effect of mixing time: 75/25 blend, (a) $t_{mix} = 10$ min; (b) $t_{mix} = 15$ min. 25/75 blend, (c) $t_{mix} = 5$ min; (d) $t_{mix} = 10$ min (e) $t_{mix} = 15$ min.

3.3. Dynamic mechanical properties

DMA data are reported at various compositions on quenched blends at $t_{mix} = 10$ min; see Figs. 7 and 8 for storage E' and loss modulus E'', respectively, and for the 75/25 and 25/75 compositions at various mixing times, Figs. 9 and 10, respectively.

As seen in Fig. 7, addition of 10 wt% PU leads to stiffening, possibly the result of intermolecular interaction of the two components. On the basis of modulus variation the blends are separated into two groups — the result of matrix inversion at the median composition. Fig. 7, inset shows the modulus variation of blends at two representative compositions, which were leached to remove PU (75/25 and 25/75).

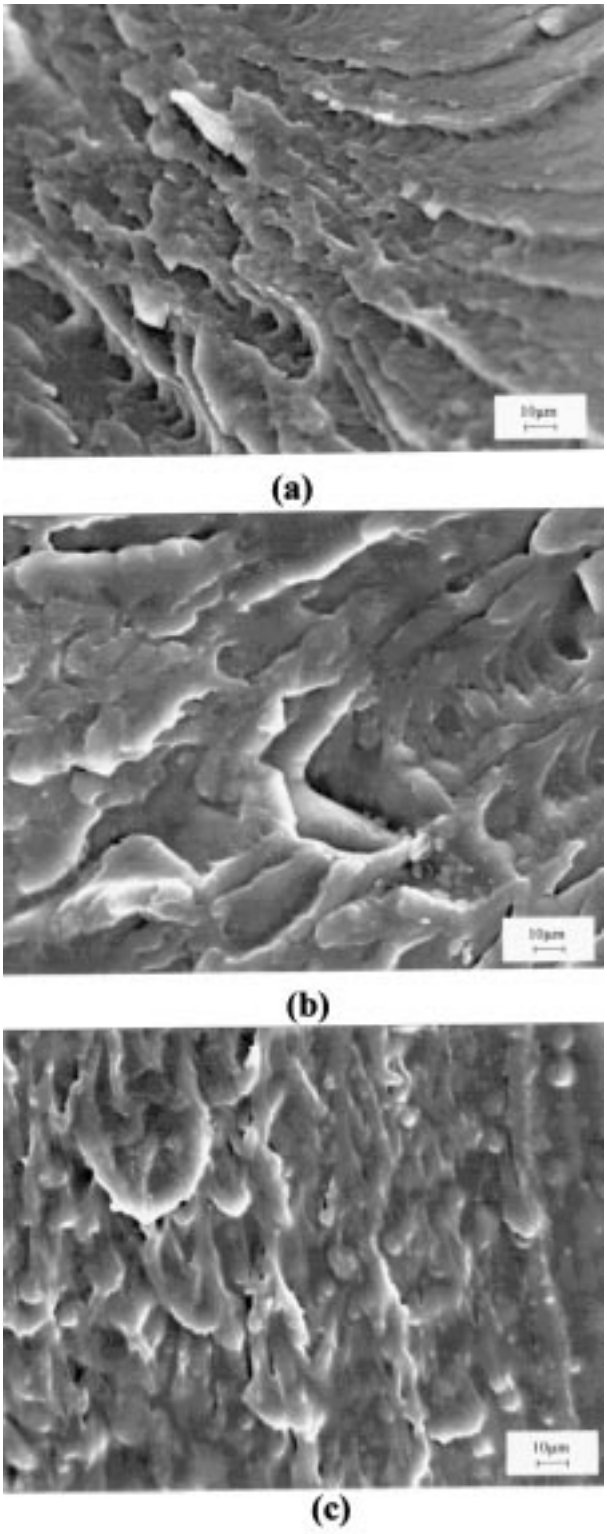

Fig. 4. SEM of cryofractured surfaces of PBT/PU blends: (a) 75/25; (b) 50/50; (c) 25/75.

The stiffness is quite different from that of PBT and reflects the formation of a modified polymer via compatibilization. This is also evident in the corresponding spectra of E'' reported in Fig. 8, inset; see below. In Fig. 8 mixing of the two components at the interface is evident from the fact that both primary T_g relaxations, of PBT (at ca. 50°C) and of PU (at ca. −20°C) are present, though converging to each other. At PU contents ≥50 wt % a single broad relaxation is observed — the result of merging of two peaks. A routine deconvolution procedure of these relaxations gave the component peaks shifted to each other. These are also reported in Table 2 in parentheses. Fig. 8, inset shows the DMA spectra of the above leached blends. The spectra show primary relaxations intermediate between those of pure components. These findings are further discussed in the last section. The effect of t_{mix} on DMA spectra is shown in Figs. 9 and 10 for the 75/25 and 25/75 blends, respectively. Increasing t_{mix} results in a progressive flexibilization of PBT (see Fig. 9), with a concomitant decrease of T_g — see inset of Fig. 9 on the E'' variation. Of interest also is the fact that at low t_{mix} (5 min) the two separate component peaks are observed and these merge into one at high t_{mix} (>10 min). This is evidence for an increased degree of compatibilization with t_{mix}. These effects are at variance with those obtained for the 25/75 blend; see Fig. 10. Indeed it is shown (inset of Fig. 10), that at increased t_{mix} the blend shows a lower degree of dispersion since the intermediate single peak moves to lower temperatures (ca. −20°C at $t_{mix} = 10$ min). These findings are generally in line with the phase-contrast microscopy, see Fig. 3, in that when two relaxations appear the phase distribution becomes coarser. Data on the main relaxations obtained for these blends as well as for annealed samples are summarized in Table 2, where thermal data have also been included. For the PU-rich blend annealing leads to considerable E' reinforcement; spectra are reported elsewhere [12]. As E'' variation and T_g component shifts indicate (see Table 2), annealing promotes phase separation.

3.4. Thermal properties

Thermal data obtained during the second heating scan are reported in Table 2. Depending on heating rate and/or thermal history pure PBT gives two close-lying melting endotherms [13]: a very small one at ca. 210°C preceding the main endotherm that is obtained by recrystallization during the second heating scan. This main T_m and the associated degree of crystallinity X_C as well as the crystallization temperature T_c are reported in Table 2. These endotherms are also obtained in annealed blends. Since crystal reorganization is hindered by PU the two endotherms observed are further apart. PU in quenched blends crystallizes slowly; therefore, during the second heating only the $T_{m,PBT}$ is observed. Since in 25/75 and 10/90 blends the T_m observed was close to that of pure PU, thermal measurements were also made on specimens leached to remove PU. The results indicated that the endotherms originally observed belong to PBT. In general, crystallization of PBT, as bulk crystallinity X_C indicates, is retarded with increasing PU content — a result expected in partially miscible polymer alloys. An

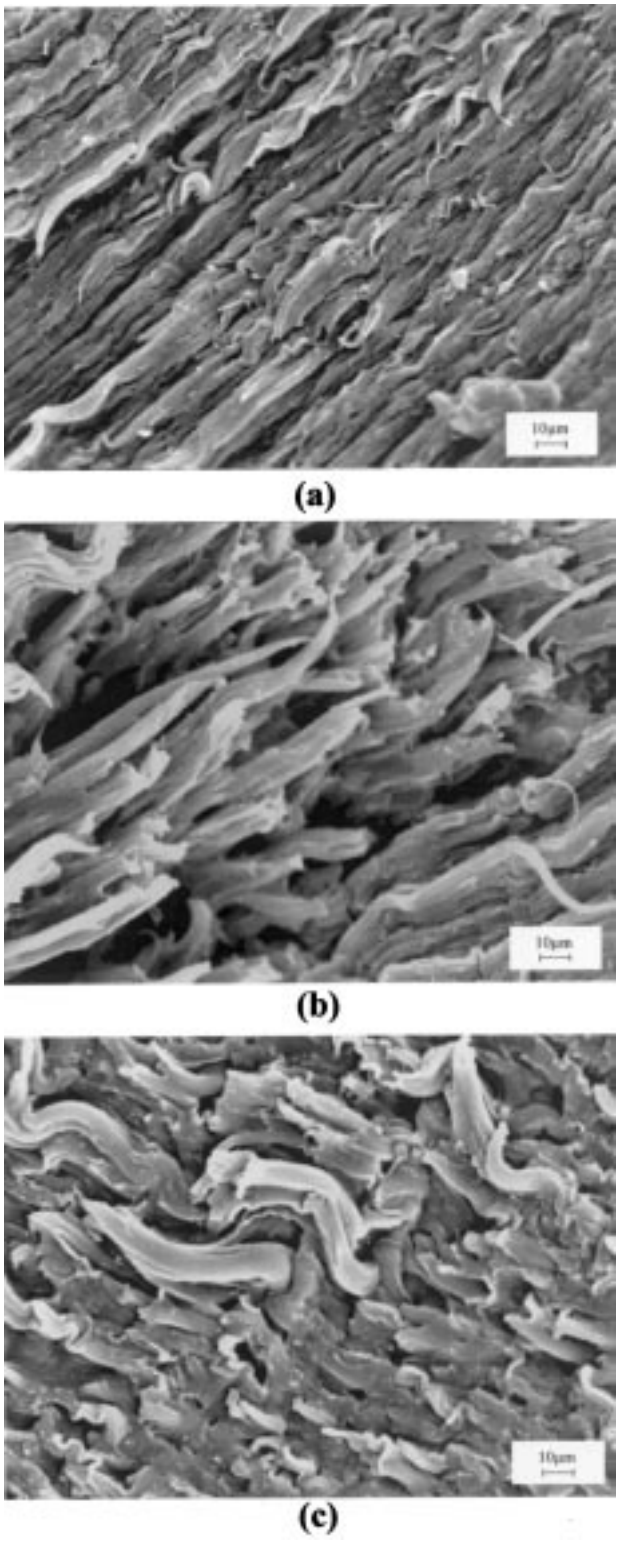

Fig. 5. SEM of PBT/PU blends fractured at ambient temperature: (a) 75/25; (b) 50/50; (c) 25/75.

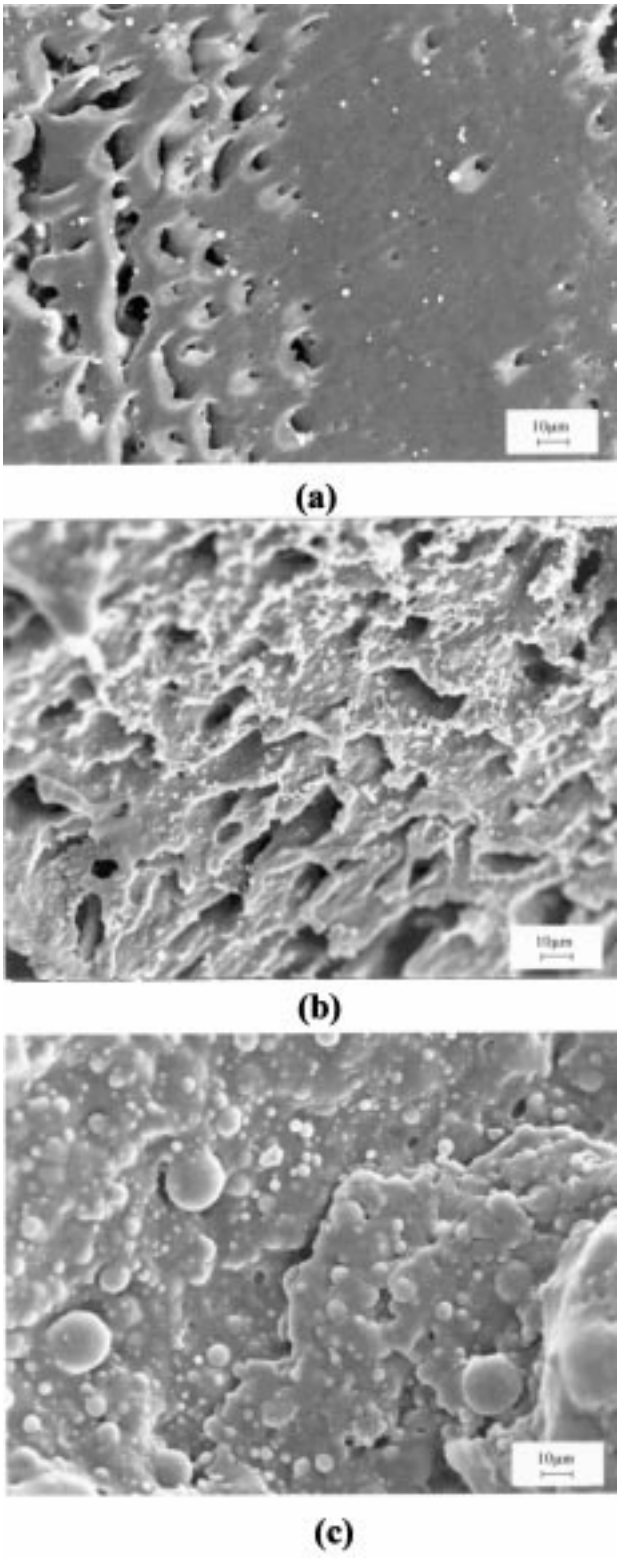

Fig. 6. SEM of etched PBT/PU blends: (a)75/25; (b) 50/50; (c) 25/75.

exception is noted for the PU-rich blends where PBT is phase separated and its crystallization is less hindered.

Except for pure PU and the annealed PU-rich blend (25/75), all T_m reported in Table 2 refer to the PBT component. Table 2 also shows the effect of annealing of a PU-rich blend and of t_{mix} in lowering $T_{m,PBT}$. Increasing t_{mix} reduces $T_{g,PBT}$ while $T_{g,PU}$ cannot be clearly defined (see Fig. 10, inset). A significant $T_{m,PBT}$ and $T_{c,PBT}$ reduction is

Table 1
Tensile properties of quenched blends

PBT/PU blends	Mixing temperature (°C)	σ_y (MPa)	σ_b (MPa)	ϵ_b (%) $\Delta L/L_0$	ϵ_b (%) $\ln(L/L_0)$	E_b (J cm^{-3})
$t_{mix} = 10$ min						
100/0	–	43 ± 5	28 ± 3	102 ± 43	69 ± 19	33 ± 9
90/10	250	33 ± 3	23 ± 2	171 ± 58	98 ± 24	43 ± 6
75/25	250	27 ± 3	36 ± 4	670 ± 108	204 ± 14	161 ± 45
75/25[a]	250	–	35 ± 2	24 ± 6	21 ± 5	7 ± 1
75/25[b]	250	32 ± 3	24 ± 5	363 ± 69	153 ± 16	76 ± 15
50/50	250	–	36 ± 3	559 ± 61	188 ± 10	172 ± 44
25/75	250	–	29 ± 2	534 ± 58	184 ± 9	89 ± 10
25/75[a]	250	–	25 ± 2	235 ± 48	120 ± 14	47 ± 11
25/75[b]	250	–	29 ± 2	447 ± 26	170 ± 5	88 ± 9
10/90	250	–	28 ± 3	511 ± 21	181 ± 3	81 ± 8
0/100	–	–	56 ± 5	807 ± 130	220 ± 14	222 ± 22
$t_{mix} = 5$ min						
75/25	250	27 ± 2	39 ± 4	701 ± 90	207 ± 12	167 ± 22
25/75	250	–	33 ± 4	522 ± 64	182 ± 11	113 ± 9
25/75[a]	250	–	27 ± 5	297 ± 80	137 ± 19	53 ± 15
$t_{mix} = 15$ min						
75/25	250	19 ± 3	30 ± 3	557 ± 65	188 ± 10	92 ± 21
25/75	250	–	30 ± 4	492 ± 63	177 ± 11	96 ± 24
25/75[a]	250	–	29 ± 3	449 ± 32	170 ± 6	121 ± 16
$t_{mix} = 20$ min						
75/25	250	11 ± 1	23 ± 3	440 ± 60	168 ± 11	57 ± 15

[a] Annealed at 140°C for 30 min.
[b] After 20 days physical aging at 25°C.

also obtained. At PU-rich compositions and increased t_{mix} (15 min) no T_m endotherms are observed. In general both T_m and T_c data obtained with increasing t_{mix} indicate a progressively less perfect crystal structure due to higher degrees of compatibilization and are in agreement with FT-IR spectral changes at increased t_{mix}; see below.

3.5. Spectroscopy

3.5.1. FT-IR

Spectra were obtained for various compositions and for the 75/25 blend at various t_{mix}.

The results are analyzed in terms of PBT crystal transformation and intermolecular interactions.

3.5.1.1. Effect on crystal structure. PBT crystallizes in two forms [14]: the a-crystal with a *g–t–g* conformation and the b-crystal (formed under stress) with a *t–t–t* conformation. Most characteristic absorptions for these crystal forms were observed and are reported elsewhere [12]; e.g. Fig. 11 shows the spectrum for the a-crystal (combination of skeleton and rocking vibrations, at 916 cm^{-1}) and of the b-crystal at 965 cm^{-1}. In all cases [12] increasing t_{mix} reduces the intensity of the a-crystal absorptions. This may be the result of destruction of the packing in the a-crystals and/or the elimination of trans and high energy (A) bond rotations [15].

3.5.1.2. Molecular interactions. Of the various absorption bands associated with inter- or intramolecular interactions, the hydrogen bonding associated with the –NH stretching vibration at 3332 cm^{-1} is of relevance to the present study (see Fig. 12). Hydrogen bonding also involves the $-O-\overset{\overset{O}{\|}}{C}-$ group from the soft segment and the $-\overset{\overset{O}{\|}}{C}-NH-$ group from the hard segment of PU. The non-associated –NH group absorbs at ca. 3450 cm^{-1}. Inspection of Fig. 12 shows that in PU practically all of the –NH– groups are hydrogen bonded. Addition of PBT disrupts the hydrogen bonded structure yielding free –NH– groups. The net result is a shift of the maximum to a higher frequency (3332 → 3352 cm^{-1}). The width of the absorption band in blends is attributed to the variety of the associated species involved, $-NH\cdots O-\overset{\overset{O}{\|}}{C}-$, –NH···O=C–O–, –NH···O=C–NH–, with the ester group of PBT. Finally the reduction in strength of this band is a result of dilution caused by the addition of polyester.

Ester–amide interchange reactions that could conceivably take place cannot be studied in these blends since in pure PU the characteristic bands of –C=O and –NH– are broad: 1675–1760, 1500–1560 and 1180–1220 cm^{-1} for the Amide I, II and III conformations, respectively, causing coupled vibrations [16]. The PBT –C=O absorption and the –C–O– stretching vibration at 1700–1750 and 1000–1120 cm^{-1}, respectively, are also broad. Thus in blends any shift due to molecular interactions would not be identifiable.

Table 2
Viscoelastic and thermal properties of blends

PBT/PU blends	High T_g (°C)	Low T_g (°C)	T_m (PBT) (°C)	T_c (PBT) (°C)	X_c (PBT) (%)[a]
$t_{mix} = 10$ min					
100/0	50	–	224	191	22
90/10	47	–	221	182	19
75/25	45	–	221	178	20
75/25[c]	48	–	213, 221	179	21
75/25[d]	[e]	[e]	219	178	25
50/50	30[f]	–	200	168	[g]
	(28)	(13)			
25/75	–	−7[f]	217	165	5
	(19)	(9)			
25/75[c]	46	−18	196 (PU)	177	12
			210, 220		
10/90	–	−13[f]	219	177	11
	(14)	(11)			
0/100	–	−20	201, 219	137, 114	26[b]
$t_{mix} = 5$ min					
75/25	47	−9	216	160	21
25/75	–	−2[f]	219	161	13
$t_{mix} = 15$ min					
75/25	38	–	194	142	18
25/75	–	0[f]	–	–	–
25/75[c]	–	2[f]	–	–	–
$t_{mix} = 20$ min					
75/25	36	–	187	149	18
Etched samples					
75/25	33[f]	–	217	175	28
25/75	50	19	219	158	6

[a] ΔH_f^0(PBT) = 33.44 cal g^{-1} [11].
[b] ΔH_f^0(PU) = 5.83 cal g^{-1} [19].
[c] After annealing at 140°C for 30 min.
[d] After 20 days physical aging at 25°C.
[e] Not examined.
[f] Broad relaxation.
[g] Merging of the two endotherms.

To obtain unequivocal information on possible intercomponent interaction, compositions 75/25 and 25/75 were examined after prolonged extraction of PU. The spectra, Figs. 13 and 14, showed the characteristic absorptions at 1535 and 1600 cm^{-1} present in PU and attributed to Amide II conformation and C=C stretching vibration of the aromatic ring, respectively. These results are in line with the DMA and NMR measurements indicating mixing at the interphase and possible copolymer formation; see below.

3.5.2. ^1H NMR

In the previous study [1] NMR gave evidence for the formation of a copolymer and a possible mechanism was proposed based on ester–amide interchange reactions. Similar results were obtained in the present work. In Fig. 15(i) of the pure PBT spectrum the single peaks at 7.74 and 4.12, 1.64 ppm, correspond to the aromatic (**a**) and aliphatic (**b**, **c**) protons, respectively. Focusing on the aromatic H in the spectrum of the 75/25 blend, (Fig. 15(ii)–(iv)), taken at progressively higher mixing times, one detects an additional peak at 7.78 ppm when $t_{mix} \geq 10$ min. The amount of copolymer formed was estimated to be 3 and 5 wt% for (c) and (d), respectively. This was not observed for the 25/75 blend at similar t_{mix} (Fig. 15(v) and (vi)).

The new peak has been attributed to the change of environment of the aromatic H due to the formation of a PU–PBT copolymer — the result of isocyanate groups from PU chemically reacting with terminal carboxyl groups of PBT; see below. Similar findings were reported by Pillon and Utracki [17] who studied melt mixed PET/PA-66 blends in the presence of a catalyst. As to why the new additional peak is not observed in PU rich blends a possible explanation is given below.

4. Discussion

Static and dynamic mechanical properties as well as

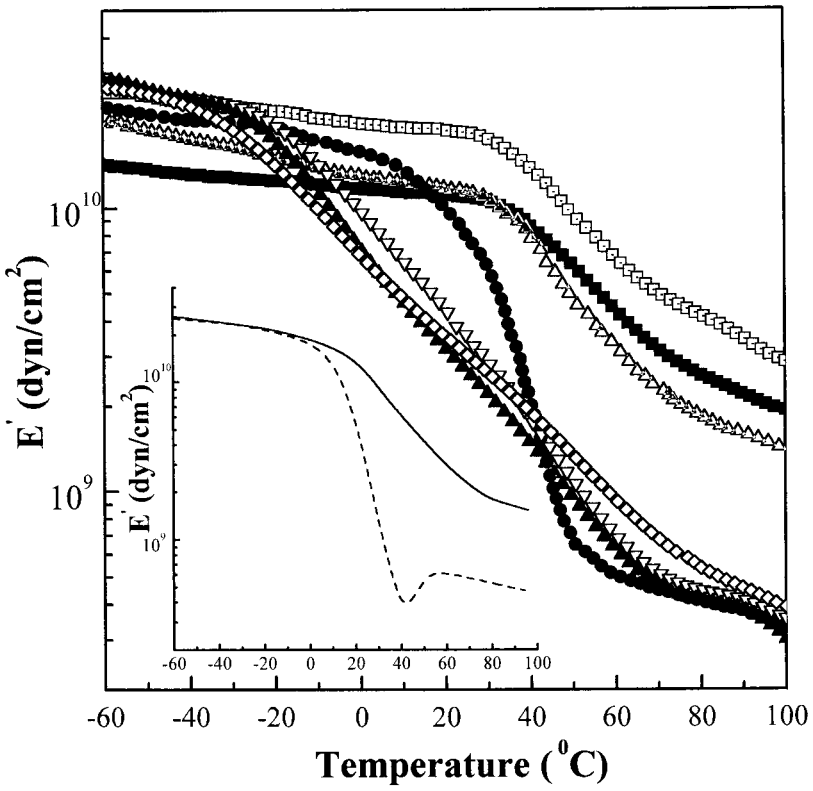

Fig. 7. Temperature dependence of storage modulus E' of PBT/PU blends: (■) 100/0; (⊡) 90/10; (△) 75/25; (●) 50/50; (▽) 25/75; (▲) 10/90; (◇) 0/100. Inset — storage modulus of leached blends: (—) 75/25; (– –) 25/75.

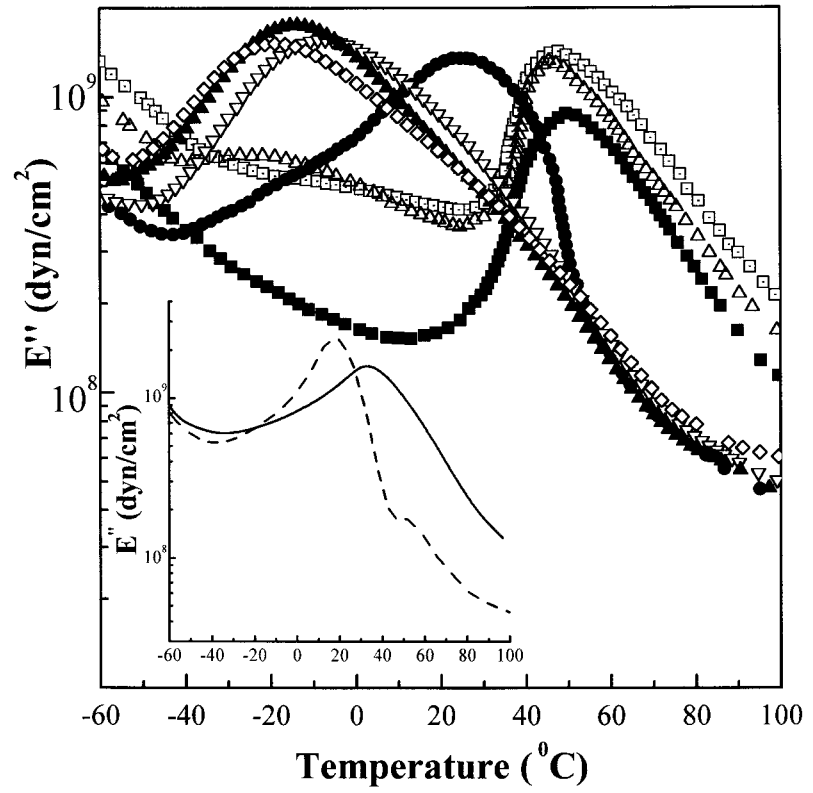

Fig. 8. Temperature dependence of loss modulus E'' of PBT/PU blends:(■) 100/0; (⊡) 90/10; (△) 75/25; (●) 50/50; (▽) 25/75; (▲) 10/90; (◇) 0/100. Inset — storage modulus of leached blends: (—) 75/25; (– –) 25/75.

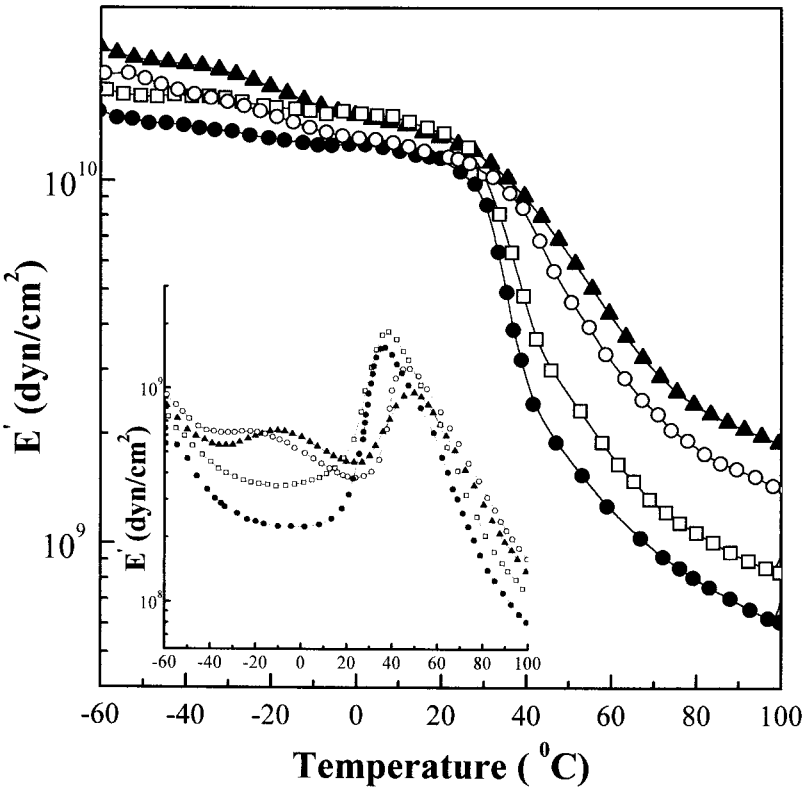

Fig. 9. Effect of mixing time on storage modulus of 75/25 blends: (-▲-) $t = 5$ min; (-○-) $t = 10$ min; (-□-) $t = 15$ min; (-●-) $t = 20$ min. Inset — loss modulus.

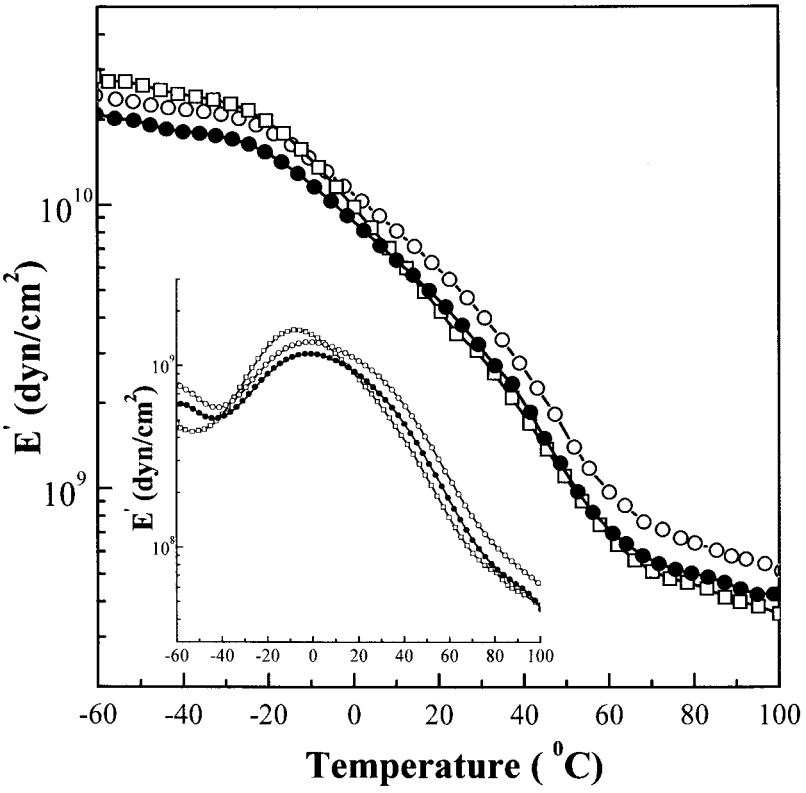

Fig. 10. Effect of mixing time on storage modulus of 25/75 blends: (-○-) $t = 5$ min; (-□-) $t = 10$ min; (-▲-) $t = 15$ min.

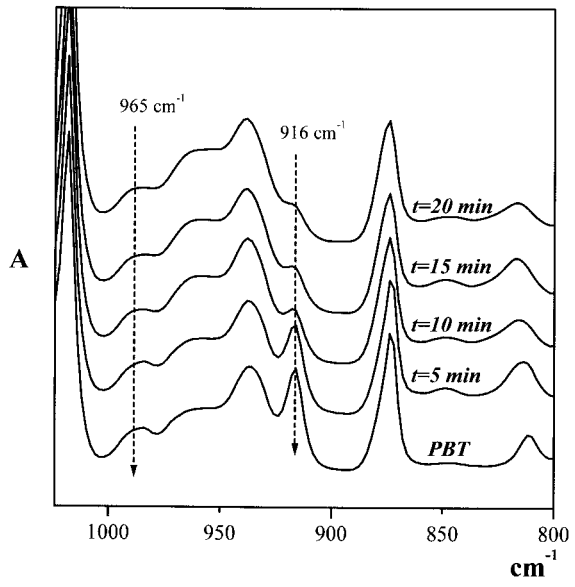

Fig. 11. FT-IR spectrum of 75/25 PBT/PU blend. Effect of mixing time.

thermal data combined with morphological features support the view that at the mixing conditions employed polymeric alloys of PBT/PU are obtained. Additional DMA data in blends where PU was selectively removed, see Fig. 8, inset, give evidence for the formation of a blend with relaxations intermediate to those of PBT and PU; 33°C for the 75/25 and 19 and 50°C (shoulder) for the 25/75 blend. If physical intermolecular interactions were responsible for the relaxations shifts observed in blends, in etched blends one would recover PBT with a main relaxation at 50°C. Thus some chemical bonding between partners is involved. Moreover, spectroscopic evidence based on FT-IR of leached

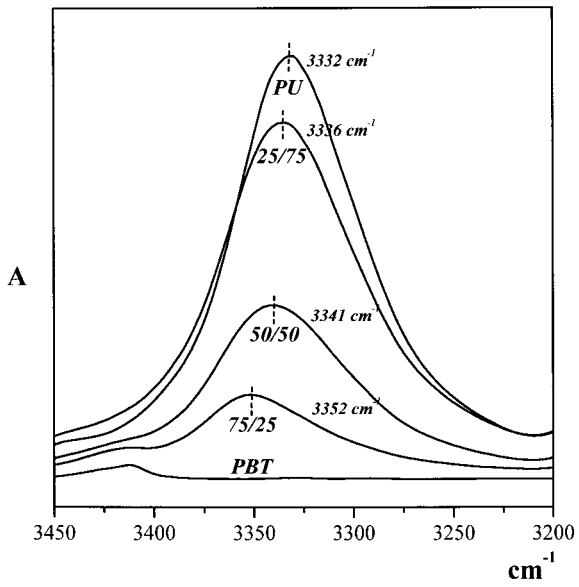

Fig. 12. FT-IR spectra of PBT/PU blends. Effect of composition.

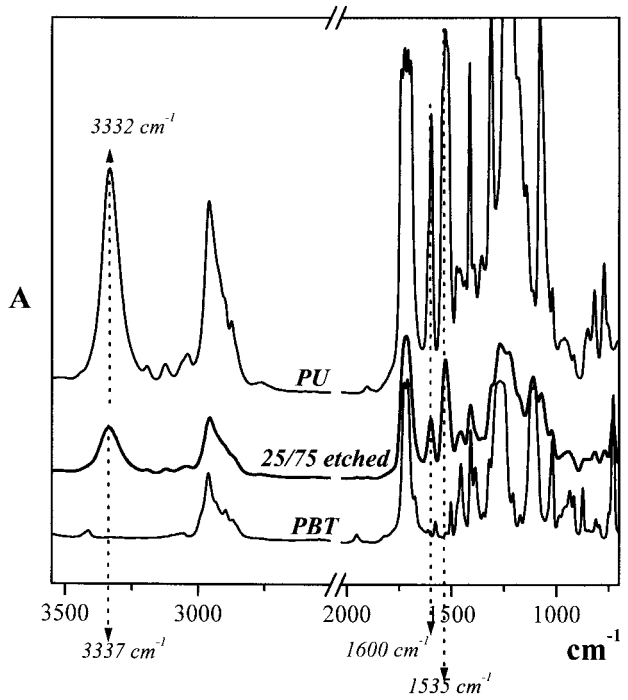

Fig. 13. FT-IR spectrum of leached 25/75 PBT/PU blend.

samples and NMR give evidence for the formation of a PBT–PU copolymer. Its presence facilitates component dispersion and subsequent reactive compatibilization when adequate mixing time is employed. In addition, interactions between the carbonyl groups of PBT and the imidic hydrogen of PU may contribute since during melt mixing

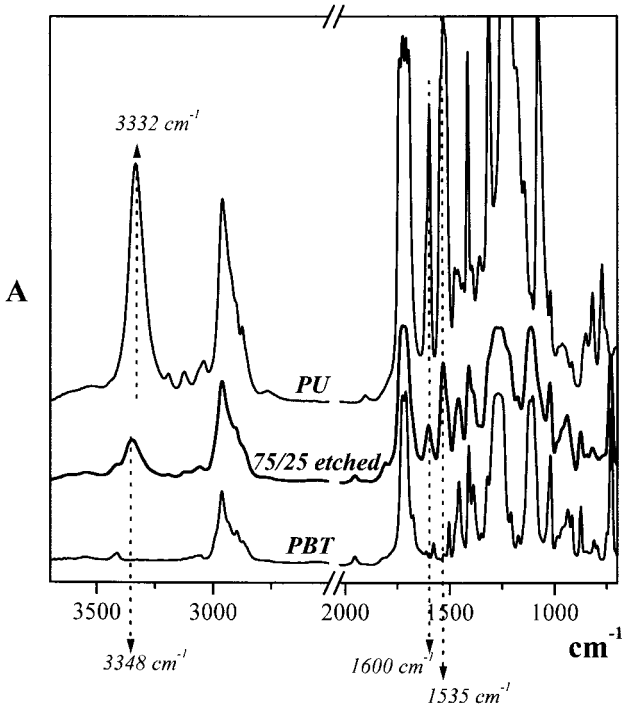

Fig. 14. FT-IR spectrum of leached 75/25 PBT/PU blend.

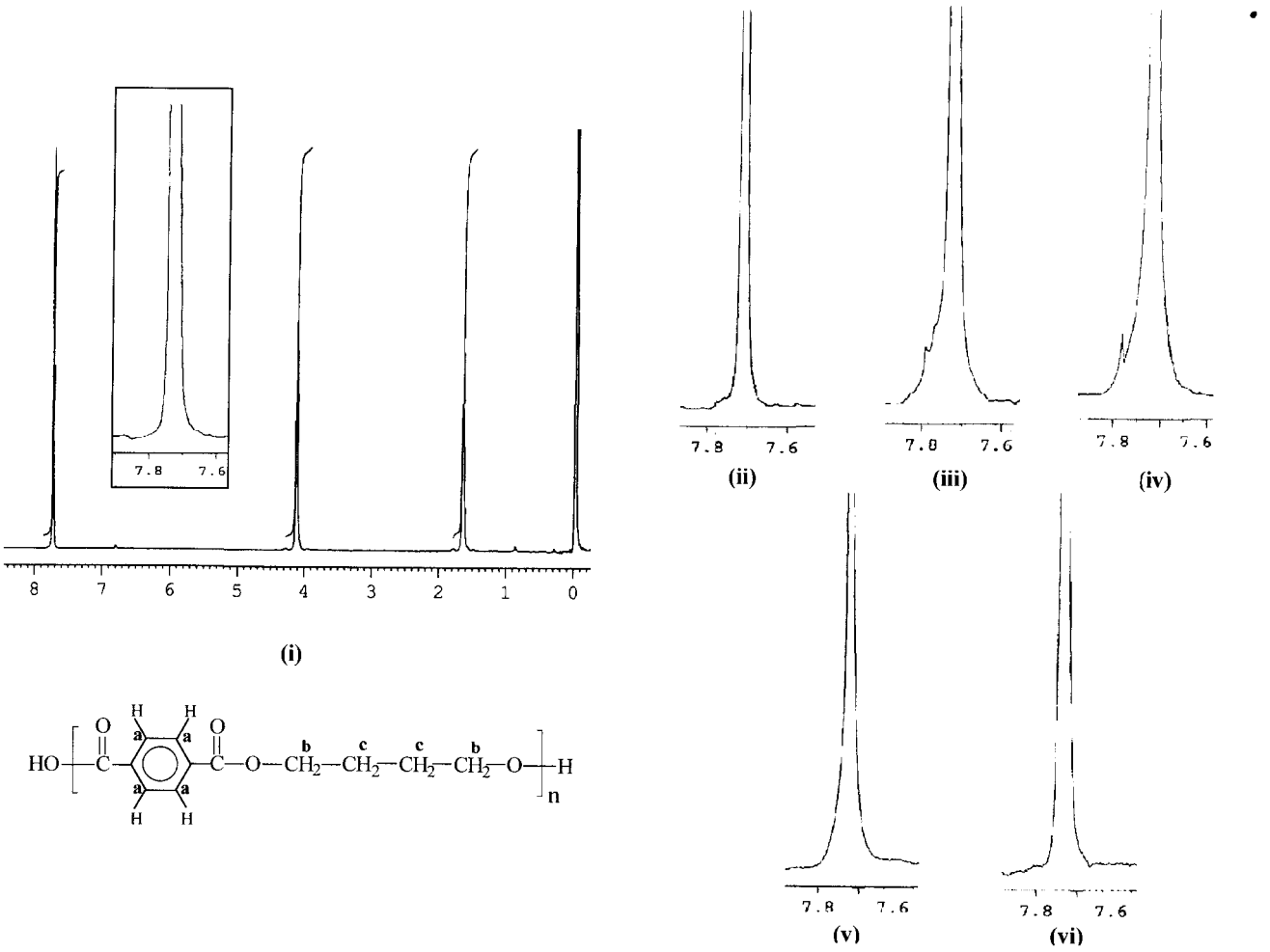

Fig. 15. NMR spectra of PBT/PU blends. Effect of composition and mixing time: (i) pure PBT; 75/25 blend, (ii) $t_{mix} = 5$ min; (iii) $t_{mix} = 10$ min; (iv) $t_{mix} = 15$ min; 25/75 blend, (v) $t_{mix} = 10$ min; (vi) $t_{mix} = 15$ min.

FT-IR results indicated disruption of the hydrogen bonded PU.

The sequence of reactions that may take place is summarized in Scheme 1. Reaction path (**a**) is reversible and takes place during the initial stage of melt mixing. The R ~ NCO chains that result from thermal dissociation may also participate in reaction paths **I** and **II** involving the terminal active groups of PBT. Reaction path **I** is slow and irreversible, involving the terminal carboxyl of PBT. This reaction leads to the modification of the NMR spectrum of the aromatic protons of PBT observed and is expected to yield measurable concentrations of copolymer **I** only at PBT-rich compositions, v.a. Reaction **II** involving the terminal hydroxyl of PBT is much faster [18] and produces copolymer **II**, which does not lead to modification of the NMR spectrum. Given the preference of the R ~ NCO to react via route **II**, it is reasonable to expect that at low PBT ratios in blends, most of it is consumed to form type **II** copolymer. Thus the concentration (if any) of copolymer **I** is too low to detect by NMR. However the FT-IR of the leached blends gives evidence for a copolymer formation — the result of reactive compatibilization by both routes **I** and **II**.

A referee suggested that transesterification reactions between PBT and the polyester soft segment phase of the PU may be possible, if a residual catalyst (used for the manufacture of PBT) is present. Though this possibility cannot be ruled out we do not have spectroscopic evidence to support it.

5. Conclusions

1. Polymeric alloys with improved mechanical properties are obtained by reactive melt blending of PBT with thermoplastic PU.
2. DMA and spectroscopic evidence support the view that during melt blending ester–amide interchange reactions take place, forming a PBT–PU copolymer. The latter promotes good component dispersion and interphase bonding via intermolecular reactions.

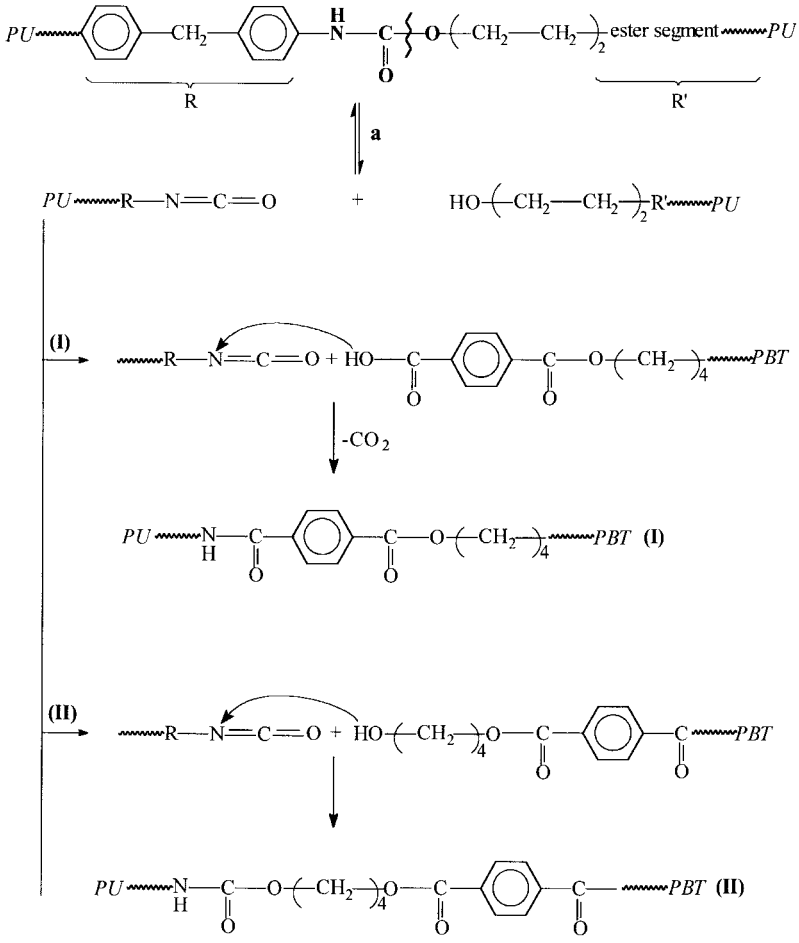

Scheme 1.

Acknowledgements

The authors thank Profs J. Kallitsis, K. Gravalos and Dr K. Samios for useful discussions. Thanks are also due to Nevicolor SpA and Bayer A.G. for providing materials and information. This work was supported in part by the Operational Programme for Education and Initial Vocational Training, Programme on Polymer Science and Technology-3.2a, 33H6, administered jointly by the Ministry of Education in Greece and the European Community (Programme JOULE 1998-2000, PL-970014).

References

[1] Samios CK, Gravalos KG, Kalfoglou NK. Eur Polym J 2000;36:937.
[2] Peterson RJ, Corneliussen RD, Rozelle LT. Polym Prepr (Am Chem Soc, Div Polym Chem) 1969;10:385.
[3] Fambri F, Penati A, Kolarik J. Polymer 1997;38:835.
[4] Ahn TO, Jung S, Lee J, Jeong HM. J Appl Polym Sci 1997;64:2363.
[5] Kim SC, Klempner D, Frisch KC, Radigan W, Frisch HL. Macromolecules 1976;9:258.
[6] Kim SC, Klempner D, Frisch KC, Frisch HL. Macromolecules 1976;9:263.
[7] Matsuo M, Kwei TK, Klempner D, Frisch HL. Polym Engng Sci 1970;10:327.
[8] Papadopoulou CP, Kalfoglou NK. Polymer 1997;38:4207.
[9] Seymour RB, Carraher CE. Structure–property relationships in polymers. New York: Plenum Press, 1984 (chap. 4).
[10] van Krevelen DW. Properties of polymers. New York: Elsevier, 1972 (p. 200).
[11] Illers KH. Colloid Polym Sci 1980;258:117.
[12] Archondouli P. MSc thesis, in preparation.
[13] Hobbs SY, Pratt CF. Polymer 1975;16:462.
[14] Hopfe I, Pompe G, Eichorn K-J. Polymer 1997;38:2321.
[15] Stambaugh BD, Koenig JL, Lando JB. Polym Lett 1977;15:299.
[16] Bellamy LJ. The infra-red spectra of complex molecules. 2nd ed. London: Methuen, 1958 (chap. 120).
[17] Pillon LZ, Utracki LA. Polym Engng Sci 1984;24:1300.
[18] Ravve A. Organic chemistry of macromolecules. New York: Marcel Dekker, 1967 (p. 295).
[19] Papadopoulou CP, Kalfoglou NK. Polymer 1998;39:7015.